Preformed pits as initiation sites for stress corrosion of austenitic stainless steels

ANTONIO ALDERISIO, BRUNO BREVAGLIERI, GIUSEPPE SIGNORELLI, Dipartimento di Ingegneria Chimica, dei Materiali, delle Materie Prime e Metallurgia, Sede Metallurgia, Facoltà di Ingegneria, Università La Sapienza, Roma.

Abstract

A study has been made of the effect of preformed pits on the corrosion behaviour of a heat-treated AISI 304 austenitic stainless steel under constant load equal to 80% of $\sigma_{p\ (0.2)}$, at polarization potentials in the imperfect passivity region and under open circuit conditions, exposed to aqueous solutions with diverse $SO_4^{=}/Cl^-$ ratios.

With polarization in the passive range and a ratio of 1/0.2, as in the first stage of stress corrosion, intergranular attack on the bottom of pits with critical dimensions has been observed. On the walls of the cracks there are characteristic signs of transgranular attack. An increase in temperature causes an increase in the rate of the phenomenon, without leading to the appearance of different forms of corrosion.

With polarization in the active range the trend of the crack is always transgranular. Sometimes the crack walls appear to be marked with fine parallel pleats, parallel grooves and micropits. In some conditions — low temperature and very small pits — the formation of martensite, attacked in a highly selective manner, prevents stress corrosion.

Riassunto

È stato studiato l'effetto di cavità preformate sul comportamento alla corrosione di un acciaio inossidabile austenitico AISI 304 solubilizzato sotto un carico costante pari all'80% di $R_{p\ (0,2)}$, a potenziali di polarizzazione compresi nell'intervallo di passività imperfetta e in condizione di libera corrosione, esposto a soluzioni acquose con diversi rapporti $SO_4^{=}/Cl^-$.

Nella polarizzazione in campo passivo e con rapporto 1/0,2, come primo stadio della tensocorrosione, è stato osservato un attacco intergranulare sul fondo di cavità con dimensioni critiche. Sulle pareti delle cricche appaiono i segni caratteristici dell'attacco transgranulare. Un aumento della temperatura provoca un aumento della velocità del fenomeno, senza far apparire forme diverse di attacco.

Nella polarizzazione in campo attivo l'andamento della cricca è sempre transgranulare. Talora le pareti delle cricche appaiono segnate contemporaneamente da pieghe parallele, solchi paralleli e microcavità. In alcune condizioni, temperatura bassa e cavità molto piccole, la formazione di martensite, attaccata in modo altamente selettivo, ha contrastato la tensocorrosione.

Introduction

Stress corrosion has been studied by many researchers. The results reported often differ because they were obtained under experimental conditions differing as regards corrosivity of the medium, state of the metal, type and magnitude of stress and consequent strain, presence of notches and polarization of the working electrode.

Load is generally applied by bending in the elastic range (bent-beam) and in the plastic range (U-bend), by tensioning at constant stress and at constant strain rate (1). The severity of stress corrosion varies with the type of stress (2), increasing when notches are present.

Austenitic stainless steels are studied in the heat-treated, sensitized and cold-worked state; in the latter case the amount of prestrain is important (3). Martensitic transformation can occur in these plastically deformed steels (4).

With regard to corrosion behaviour, numerous authors (5-10) and others cited thereby have reported transgranular stress corrosion of austenitic steels in the active state, under open circuit conditions or at anodic potentials in the active region.

When studying stress corrosion of Fe-Cr-Ni austenitic alloys with active behaviour in boiling $MgCl_2$, Smith & Staehle (6) observed an increase in time to cracking when O_2 is blown into the solution; they conclude that the introduction of oxygen may well favour the formation of a mechanically stronger passive film. Engseth and Scully (11) have studied repassivation behaviour of an austenitic stainless steel in medium with Cl^- ions, through measurement of the repassivation constant β, adopted as the criterion for evaluation of passive film stability. They found a decrease in the β value, indicating slower repassivation, at the lower extremity of the passive region (where the potential is close to the passive/active transition region) and at the upper extremity (close to the critical breakdown potential). They conclude that stress corrosion cracking might be encountered in these two regions of potential where β is changing rapidly. Parkins (12) comes to a similar conclusion.

Acello & Green (5) report periodic current surges at potentials slightly above E_{pp}, the primary passive potential. This leads them to suspect that stress corrosion may occur in that region of potential, despite the fact that no cracking was observed within three days when polarizing the alloys at such potentials.

According to Hehemann (13) stress corrosion may occur in a metal/environment system when the stationary corrosion potential, which is intimately related to the breakdown potential in the case of an austenitic stainless steel, is noble to the critical cracking potential that is also the repassivation potential. In other words, where austenitic stainless steels are concerned, the cracking potential is that for termination of the localized corrosion process by repassivation.

Under normal service conditions stainless steels are exposed to environments in which they become passive, since they are in the heat-treated state, having been cold worked in a controlled manner and subjected to nominal elastic stresses.

Furthermore it is often found in industrial practice that

stress corrosion starts when pitting and crevice corrosion are active, since the pits and crevices act as stress raisers that favour crack nucleation (14). The evolution of the pits in stress-corrosion cracks has been observed during various investigations (12, 15-17). The question must be posed, however, as to whether stress intensification at the base of the pit or electrochemical conditions within the pit are the most important as regards cracking (12). A plasticized zone has been discovered at the bottom of notches where the value of the nominal stress is greatly increased (18).

Studies have also been made of the effect of sulphide inclusions on the susceptibility of steels to pitting corrosion, stress corrosion and hydrogen embrittlement (19).

These considerations justify the study of the effect of preformed pits on the corrosion behaviour of an austenitic stainless steel under constant load equal to 80% of $\sigma_{p\ (0.2)}$, at polarization potentials within the imperfect passivity range of the steel in an environment characterized by the presence of a passivating and a depassivating species; this is a methodology that has already been applied (20).

Materials and equipment

The experiments were run on small cylindrical specimens having a useful length of 40 mm and a diameter of 4 mm, cut from 10 mm diameter bar of AISI 304 austenitic stainless steel whose percentage composition is: C 0.041, Mn 1.05, Si 0.50, Cr 18.60, Ni 8.30, P 0.003, S 0.005 and Mo 0.35.
After machining, the specimens were heat treated at 1050°C and water-quenched. The oxide layer and the chromium-depleted steel layer were then removed by emery paper and the final surface finish was ensured using wet SiC 1000 paper.

H_2SO_4 + NaCl test solutions were prepared with various $SO_4^{=}/Cl^-$ ratios, namely 5/0.5, 5/0.2, 2.5/0.5, 2.5/0.2, 0.5/0.1 and 1/0.2 (all concentrations are expressed in terms of normality). The solutions were thermostated at room temperature, 70 and 90°C.

In the electrochemical tests the cell consisted of a cylindrical Pyrex container closed with a neoprene stopper through which was passed the specimen. The cell was complete with a platinum-wire counter-electrode and a Luggin capillary connected to a saturated calomel electrode (SCE). The electrochemical tests were performed with an AMEL Corrograph model 561 B. After the tests the specimens were examined under a Cambridge 600 Scanning Electron Microscope (SEM).

Methodology and experimental results

Cyclical polarization curves were run at the various temperatures selected to determine the critical breakdown potential E_R, and the protection potential E_P, under a constant tensile load equal to 80% of $\sigma_{p\ (0.2)}$.

The samples were polarized at potentials more noble than E_R to attain a current density such as to create on the surface minipits with clearly-defined geometry. In the subsequent phase of polarization at predetermined potentials these minipits acted as initiation sites in the imperfect passivity region of the steel.

This methodology takes account of the importance of the imperfect passivity region when there are pre-existing geometrical discontinuities (12).
Tests were run using aqueous solutions with different $SO_4^{=}/Cl^-$ ratios.

Under the selected conditions, with ratios of 5/0.5 and 5/0.2 no localized corrosion of any form occurred at room temperature or at 70 or 90°C. However, with solutions having ratios of 2.5/0.5 and 0.5/0.1 pitting corrosion configurations non attributable to stress corrosion were obtained, but these were always sustained by applied load, as was observed for the 1/0.5 ratio in the research cited (20).
Fig. 1 concerning a test with a 2.5/0.5 ratio illustrates

Fig. 1 - $SO_4^{=}/Cl^-$ ratio equal to 2.5/0.5, polarization in the imperfect passivity region, room temperature; micropit corrosion in a preformed pit; g = 1280.

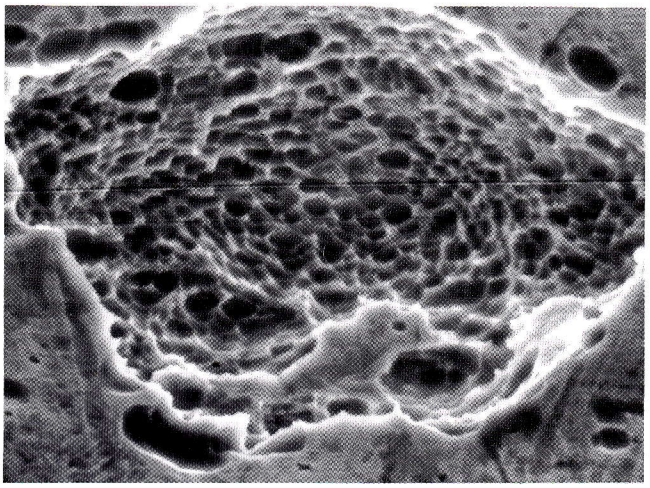

Fig. 2 - (a) Ratio 0.5/0.1, polarization in the imperfect passivity region, room temperature; pit with metal residues in platelet form; g = 70; (b) as for (a), g = 360.

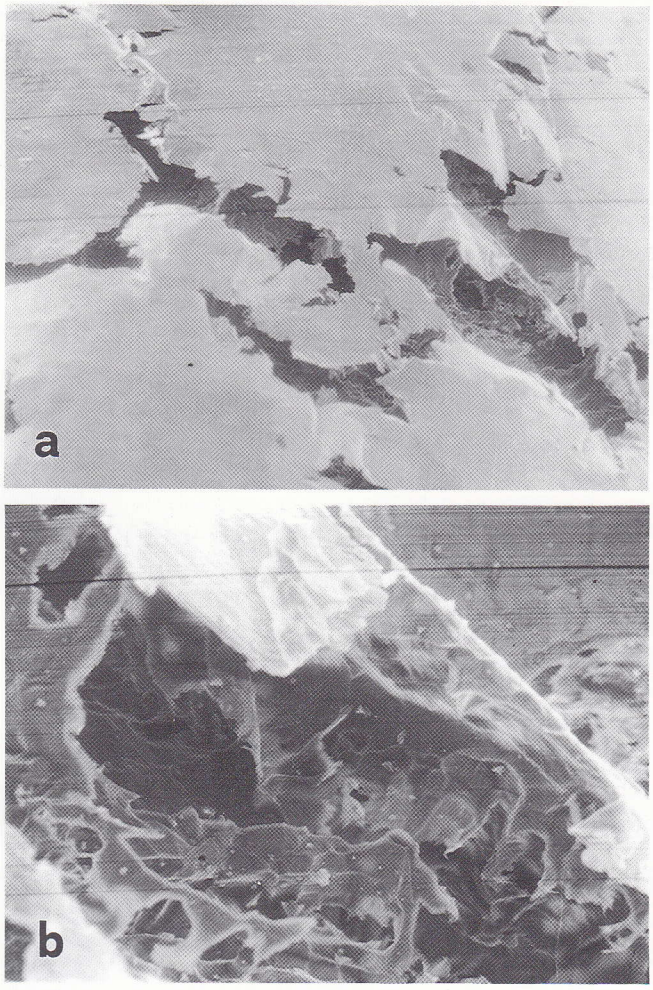

Fig. 3 - Ratio 1/0.2, polarization in the imperfect passivity region, exposure time 40-60 h, room temperature; intergranular attack on bottom of a preformed pit; g = 720.

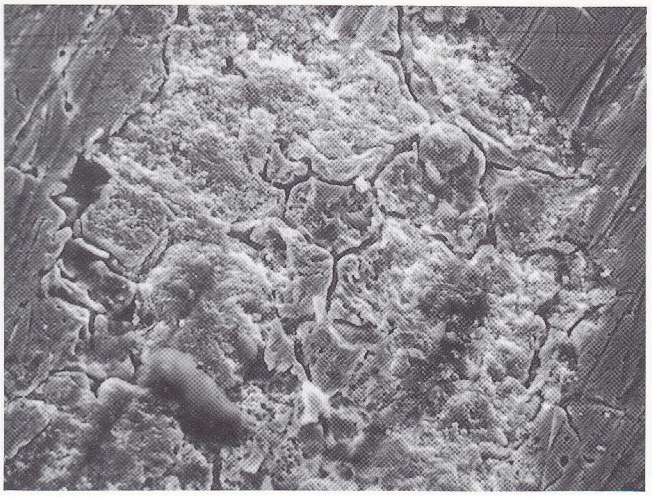

Fig. 4 - As per Fig. 3, 4 h, 70°C, intergranular attack on bottom of a preformed pit; g = 150.

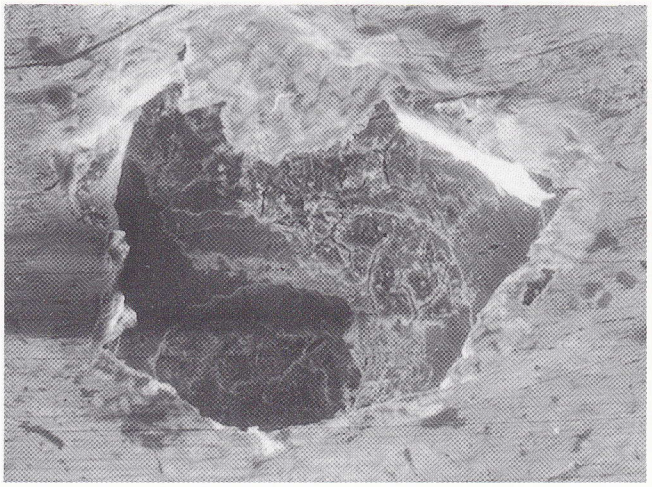

Fig. 5 - As per Fig. 4, 90°C; intergranular attack on bottom of a preformed pit, oblique section; g = 710.

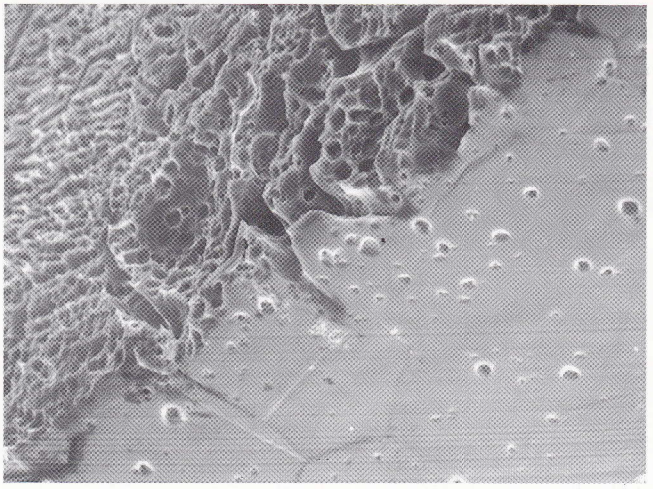

Fig. 6 - As per Fig. 3, 40 h, 90°C; advance of intergranular attack on bottom of preformed pit, oblique section; g = 185.

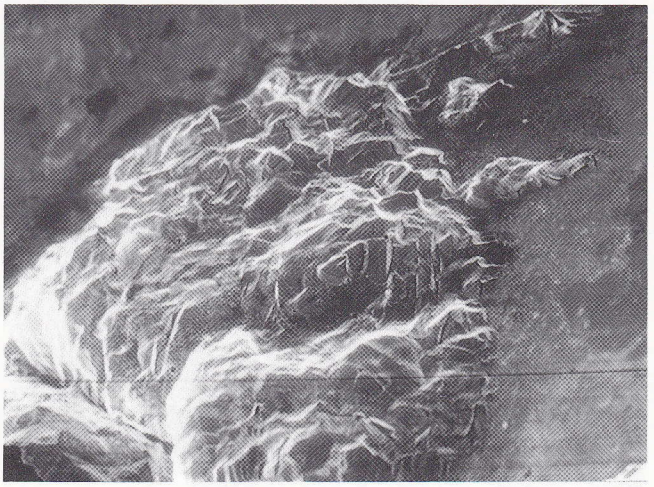

micropitting corrosion in the preformed pits, while Fig. 2 relating to tests with an 0.5/0.1 ratio indicates a pit with metallic residues in platelet form.

A completely different situation is found with a 1/0.2 ratio at room temperature after 40 and 60 hours exposure at a constant potential of + 850 mV, namely intergranular attack on the bottom of the pits, as illustrated in Fig. 3. Under identical conditions, but with 20 h exposure no form of attack was apparent. The tests conducted at 70 and 90°C, too, with 4 h exposure at a potential of + 20 mV, always within the imperfect passivity region, resulted in intergranular corrosion on the bottom of the pits (Figs 4 and 5). Fig. 6 shows the gradual advance of intergranular attack under the same experimental conditions and for exposure times prolonged up to 40 h. Examination of the crack walls reveals corrosion of the fine parallel pleats type; this is barely noticeable in the experiments at 70°C (Fig. 7a) but is much more evident in those at 90°C (Fig. 7b). In a case where, under the preceding conditions, mechanical fracture of the test specimen occurred owing to thinning of the section, the crack trend became transgranular and the crack walls exhibit a fine parallel pleat pattern in the zone of transition from corrosive to mechanical fracture (Fig. 8).

Only in the case of 1/0.2 and 0.5/0.1 ratios were tests also conducted in the active range under open circuit conditions and at anodic potentials (about − 350 mV), the results for the other ratios being already known from the literature. In the experiments conducted at room temperature and for times of up to 90 h, parallel groove attack figures are to be seen on the bottom of the pit (Fig. 9). At 90°C and an exposure time of 20 h, stress-corrosion cracks are formed; these originate mainly on the bottom of the pit (Fig. 10). Attack at the tip of one of these cracks is illustrated in Fig. 11, where a fine parallel pleat pattern characteristic of transgranular corrosion is recognizable. With polarization in the active range, even in the cases where mechanical fracture occurred owing to thinning of the section, the crack trend is constantly transgranular (Fig. 12).

Fig. 7 - (a) as per Fig. 3, 20 h, 70°C; intergranular attack with barely marked fine parallel pleat pattern; g = 620; (b) as per Fig. 3, 90°C; intergranular attack with fine parallel pleat pattern; g = 920.

Fig. 8 - As per Fig. 5; transgranular trend of crack close to mechanical fracture region; g = 900.

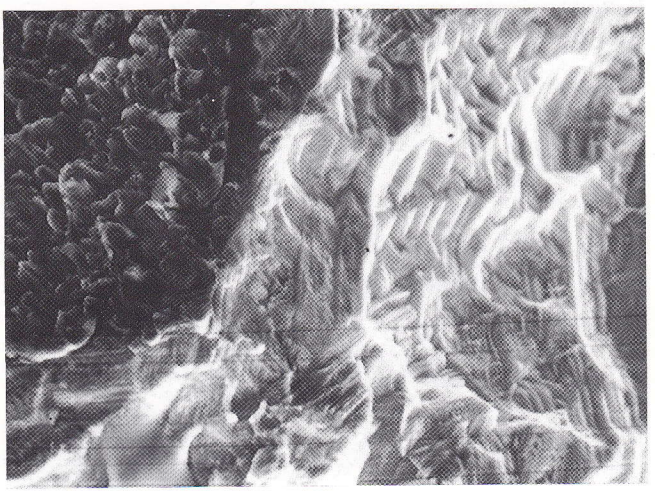

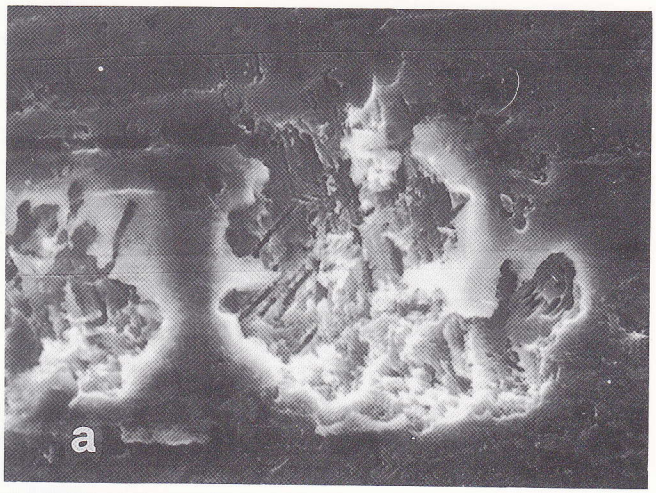

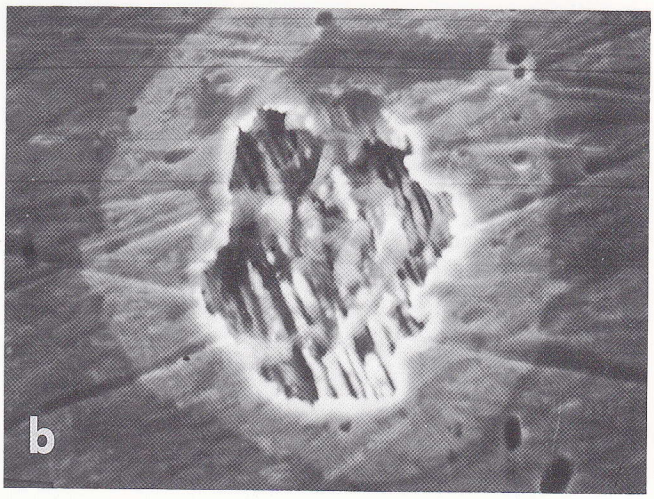

Fig. 9 - Ratio 1/0.2, polarization in active range, 90 h, room temperature; transgranular attack on bottom of a pit, parallel groove attack; (a) g = 3300; (b) as before; g = 1600.

Fig. 10 - As per Fig. 9, 20 h, 90°C, transgranular crack on bottom of a pit; g = 750.

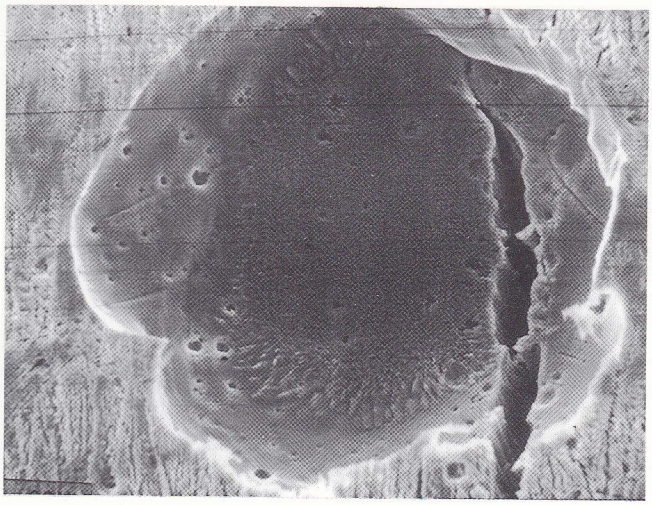

Fig. 11 - As per Fig. 10; crack tip; g = 1450.

Fig. 12 - As per Fig. 10; transgranular crack trend with fine parallel pleat pattern and parallel groove attack; g = 730.

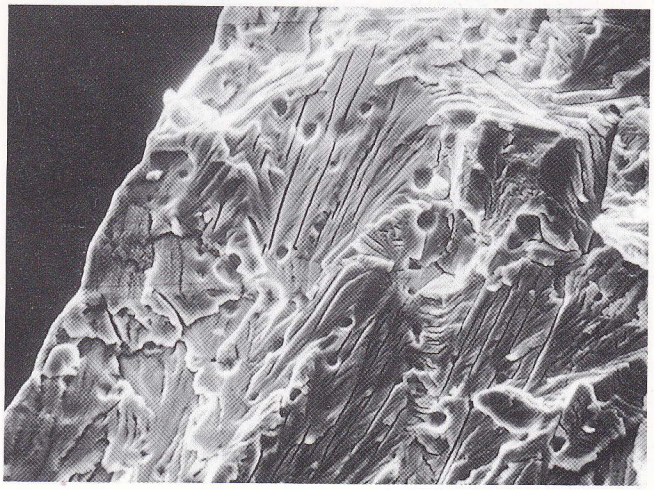

Discussion of results

In the tests performed in the passive range with $SO_4^{=}/Cl^-$ ratios of 5/0.5, 5/0.2, 2.5/0.5 and 0.5/0.1, none of the forms typical of stress corrosion were seen. Harston & Scully (7), however, operating with U-bend specimens in the active range, have observed intergranular attack with the higher ratios at least, but solely in the outer layer of grains. Attack subsequently developed to become transgranular. This can be ascribed to the different strain state and also to the diverse behaviour of the $SO_4^{=}$ and Cl^- ions in the active and passive ranges. In fact, while the Cl^- ions act as inhibitors in the active range, there is the passivating effect of the $SO_4^{=}$ ions and the penetrating effect of

the Cl^- ions in the passive range. The ratios utilized by other authors for the active range were not considered in the research reported here. In fact, no form of localized corrosion has been observed with 5/0.5 and 5/0.2 ratios in the passive range owing to the marked prevalence of the passivating species, while for 2.5/0.5 and 0.5/0.1 ratios the corrosion encountered can be ascribed to a high concentration of Cl^- ions (Figs 1 and 2). These corrosion forms occur when the corrosion rate on the walls of the site in which corrosion is localized prevails over the passivation rate; under such conditions corrosion takes the form of pitting rather than stress corrosion cracking.

With a 1/0.2 ratio, intergranular stress corrosion occurs in the imperfect passivity range, as documented by Figs 3 to 6. In this case the rate of formation of the passive film and the rate of dissolution of the steel are comparable.
When the two rates are in equilibrium, propagation of the stress corrosion crack occurs under the influence of two competitive processes: a) formation of slip steps; b) dissolution of the slip steps (21, 22).

The rate of formation of the slip steps depends on the dynamic strain rate and the stress applied in the constant load test, while the rate of corrosion of the slip steps depends on the corrosivity of the environment (7).
Under slow strain rate conditions, the formation of slip steps is slow, so this controls the overall rate. On the contrary, at high strain rates the rate of formation prevails over that of corrosion of the freshly emergent steps; so this becomes the rate controlling step in the stress corrosion cracking. The intermediate strain rates, where the rates of the two partial processes are comparable, are the most favourable for stress corrosion (22).

When the rate of formation of the slip steps is just slightly higher than the dissolution rate of the steps, a concentration of dislocations is created on the grain boundaries leading to a concentration of forces and hence to intergranular dissolution (22). It seems that intergranular fracture initiates when there is a weak corrosive environment such as low temperature and the supply of aggressive ions Cl^- to the sharp and narrow crack tip is insufficient: this tends to occur with increasing applied stress and a reduction in test temperature, and depends on alloying elements (23).

Taken as a whole, these conditions can be defined as weakly corrosive, because although the environment is strongly acid on the one hand, on the other it is characterized by a good balance between passivating and penetrating species. Such conditions have been achieved by applying a load close to the upper limit of elastic behaviour — which is intensified on the bottom of the preformed pits causing slippage of the dislocations and the blockage thereof on the boundaries — and by utilizing an environment (composition and anodic polarization) which depresses attack on the slip planes within the grains while permitting that which is localized on the boundaries.

Intergranular attack does not occur on the bottom of all the pits formed. The probable reason for this is because the pits in the imperfect passivity range tend to increase in size rather than in number. It thus seems reasonable to assume that after a given period of time not all of them manage to attain the right conditions and geometry to permit onset of intergranular stress corrosion.

Though the cracking trend is intergranular the walls of the crack are marked by corrosion figures characteristic of transgranular cracking. These figures are indicated by Nakayama & Takano (24) as having fine parallel pleat pattern and parallel groove attack, the former being characteristic of low stress levels — when crack propagation occurs mainly by preferential dissolution of active slip planes containing moving dislocations — while the latter is characteristic of high stress levels and can be attributed to a selective dissolution of martensite phases.

The morphology of the two types of corrosion is different. The fine parallel pleat pattern observed on the walls of the intergranular crack in the research reported here consists of wavy parallel lines (clearly visible at a magnification of 1000x) the trend of which varies at grain and twin boundaries. The parallel groove attack, observed during the present experiments on specimens polarized in the active range (see further on), and in the previous experiments (20) on specimens polarized in the imperfect passivity range, propagates across the grains along (111) planes (25) where the martensite has formed, leaving sharp, straight marks.

The cracks start from the bottom of the pits, as they do in the experiments conducted in the active field at 90°C (Fig. 10). In experiments run at room temperature, grooves which can be attributed to selective dissolution of the products of martensitic transformation can be seen on the bottom of the pits (Fig. 9). In fact, when high strain levels are involved, as in the case of the prestrained specimens or in the points where the stress intensification factor is very high, there is the possibility of the formation of ε and α' phase martensite, and the dissolution thereof (4).

It should be noted that the average diameter of the Fig. 9 pit is about 0.01 mm, against about 0.1 mm for the Fig. 10 pit. Formation of a martensite phase in the first

case and its absence in the second is explained by the smaller size of the Fig. 9 pit, resulting in higher stress intensification, together with the lower temperature and the smaller amount of stacking faults energy. The competitivity between selective dissolution of the martensite and stress corrosion explains why stress corrosion was prevented in the first case (4).

At higher temperatures — 70 and 90°C — the environment is more favourable for transgranular cracking. Indeed, a fine parallel pleat pattern is to be seen on the walls and at the crack tip (Fig. 11) and sometimes there are both forms of corrosion with barely-marked parallel grooves and micropits (Fig. 12).

Mixed attack (intergranular and transgranular) and transgranular attack have been observed respectively on the crack walls (Fig. 7) and near the mechanically fractured region (Fig. 8) even in the passive range. This situation can be explained by an increase in load to values close to those of fracture, with the result that slip steps appear on the surface.

In the active range, instead, corrosion is always transgranular up to the mechanically fractured region. Fig. 13 exhibits two different zones: one with ductile fracture and dimples due to overload and the other with fine parallel pleat pattern.

It is evident from the foregoing that in the environments examined, the pits represent stress corrosion initiation points whether the steel is in the active range or the imperfect passivity range. The forms of corrosion, however, differ.

Fig. 13 - As per Fig. 10; transgranular crack pattern and ductile fracture with dimples; g = 150.

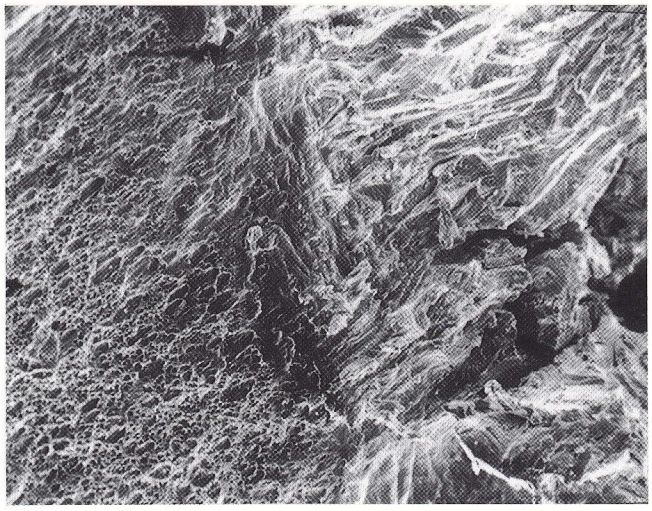

Conclusions

In a heat-treated AISI 304 stainless steel with preformed pits, exposed to H_2SO_4 + NaCl solutions, anodically polarized in the imperfect passivity region and stressed by a constant tensile load equal to 80% of $\sigma_{p\,(0.2)}$, intergranular cracking on the bottom of the pit (affecting the outermost layer) has been observed as the first stage of stress corrosion under certain conditions ($SO_4^{=}/Cl^-$ ratio of 1/0.2). Intergranular cracking occurs only in those pits which attain certain dimensions owing to the effect of anodic polarization.

Fine parallel pleats and parallel grooves characteristic of transgranular corrosion occur on the crack walls. Higher temperature influence the rate at which the phenomenon takes place but do not induce other forms of corrosion. When mechanical fracture occurs due to overload because of the thinning of the specimen, a transgranular crack trend is observed in the mechanically fractured region.

In the polarization tests in the active range the crack trend is always transgranular; moreover, the coexistence of both forms of corrosion characteristic of this trend has sometimes been encountered. Under some conditions (room temperature and very small pits) there is selective dissolution of the martensite whose formation has prevented cracking.

The conditions in which the selected steel has been examined in the research reported here are close to those which are often encountered in reality.

REFERENCES

(1) W.H. Ailor, **Handbook on Corrosion Testing and Evaluation**, Wiley, 1971.

(2) H.W. Hayden, S. Floreen, **Corrosion, 27** (10), 429-433, 1971.

(3) P. Muraleedharan, H.S. Khatak, J.B. Gnanamoorthy, P. Rodriguez, **Met. Trans. A, 16 A**, 285-289, 1985.

(4) H.E. Hänninen, **Int. Met. Reviews**, (3), 85-135, 1979.

(5) S.J. Acello, N.D. Greene, **Corrosion, 18** (8), 286t-290t, 1962.

(6) T.J. Smith, R.W. Staehle, **Corrosion, 23** (5), 117-125, 1967.

(7) J.D. Harston, J.C. Scully, **Corrosion, 25** (12), 493-501, 1969.

(8) G. Bianchi, F. Mazza, S. Torchio, **Corr. Sci., 13**, 165-173, 1973.

(9) S. Torchio, **Corr. Sci., 20**, 555-561, 1980.

(10) I. Maier, J.R. Galvele, **Corrosion, 36** (2), 60-66, 1980.

(11) P. Engseth, J.C. Scully, **Corr. Sci., 15**, 505-519, 1975.

(12) R.N. Parkins, **Met. Techn., 9**, 122-129, 1982.

(13) R.F. Hehemann, **Met. Trans. A, 16 A**, 1909-1923, 1985.

(14) Z. Szklarska-Smialowska, **Films and Their Importance in the Nucleation of Stress Corrosion Cracking in Stainless Steel**, from Hydrogen Embrittlement and Stress Corrosion Cracking, ed. R. Gibala and R.F. Hehemann, 207-229, ASM, 1984.

(15) A.A. Seys, M.J. Brabers, A.A. Van Haute, **Corrosion, 30** (2), 47-52, 1974.

(16) Z. Szklarska-Smialowska, J. Gust, **Corr. Sci., 19**, 753-765, 1979.

(17) G. Cragnolino, L.F. Lin, Z. Szklarska-Smialowska, **Corrosion, 37** (6), 312-320, 1981.

(18) T. Misawa, **Corrosion, 37** (7), 427-428, 1981.

(19) Z. Szklarska-Smialowska, E. Lunarska, **Werk. Korr., 32**, 478-485, 1981.

(20) A. Alderisio, M. Bianchi, B. Brevaglieri, G. Signorelli, **Met. Sci. Techn., 6** (1), 3-6, 1988.

(21) M. Takano, S. Shimodaira, **Trans. Japan Inst. Metals, 9**, 294-301, 1968.

(22) M. Takano, **Corrosion, 30** (12), 441-446, 1974.

(23) H. Okada, Y. Hosoi, S. Abe, **Corrosion, 27** (10), 424-428, 1971.

(24) T. Nakayama, M. Takano, **Corrosion, 38** (1), 1-9, 1982.

(25) A. Honkasalo, **Corrosion, 29** (6), 237-240, 1973.